



Inhibitory effects of selected cannabinoids against dipeptidyl peptidase IV, an enzyme linked to type 2 diabetes

Lithalethu Mkabayi^a, Zenobia Viljoen^b, Rui W.M. Krause^c, Kevin A. Lobb^c, Brett I. Pletschke^a, Carminita L. Frost^{b,*}

^a Department of Biochemistry and Microbiology, Rhodes University, Makhanda, 6140, South Africa

^b Department of Biochemistry and Microbiology, Nelson Mandela University, Port Elizabeth, 6031, South Africa

^c Department of Chemistry, Rhodes University, Makhanda, 6140, South Africa

ARTICLE INFO

Keywords:

Cannabinoids
Dipeptidyl peptidase IV
Inhibition
Type 2 diabetes

ABSTRACT

Ethnopharmacological relevance: In recent times the decriminalisation of cannabis globally has increased its use as an alternative medication. Where it has been used in modern medicinal practises since the 1800s, there is limited scientific investigation to understand the biological activities of this plant.

Aim of the study: Dipeptidyl peptidase IV (DPP-IV) plays a key role in regulating glucose homeostasis, and inhibition of this enzyme has been used as a therapeutic approach to treat type 2 diabetes. However, some of the synthetic inhibitors for this enzyme available on the market may cause undesirable side effects. Therefore, it is important to identify new inhibitors of DPP-IV and to understand their interaction with this enzyme.

Methods: In this study, four cannabinoids (cannabidiol, cannabigerol, cannabinol and Δ^9 -tetrahydrocannabinol) were evaluated for their inhibitory effects against recombinant human DPP-IV and their potential inhibition mechanism was explored using both *in vitro* and *in silico* approaches.

Results: All four cannabinoids resulted in a dose-dependent response with IC_{50} values of between 4.0 and 6.9 $\mu\text{g}/\text{mL}$. Kinetic analysis revealed a mixed mode of inhibition. CD spectra indicated that binding of cannabinoids results in structural and conformational changes in the secondary structure of the enzyme. These findings were supported by molecular docking studies which revealed best docking scores at both active and allosteric sites for all tested inhibitors. Furthermore, molecular dynamics simulations showed that cannabinoids formed a stable complex with DPP-IV protein via hydrogen bonds at an allosteric site, suggesting that cannabinoids act by either inducing conformational changes or blocking the active site of the enzyme.

Conclusion: These results demonstrated that cannabinoids may modulate DPP-IV activity and thereby potentially assist in improving glycaemic regulation in type 2 diabetes.

Abbreviations: 3D, Three-dimensional; ANOVA, One-way analysis of variance; CBD, Cannabidiol; CBG, Cannabigerol; CBN, Cannabinol; CD, Circular Dichroism; DM, Diabetes mellitus; DPP-IV, Dipeptidyl peptidase IV; GIP, Dependent insulinotropic polypeptide; GLP-1, Glucagon-like peptide 1; Gly-Pro-pNA, Gly-Pro-p-nitroanilide; MD, Molecular dynamics; PCA, Principal component analysis; PDB, Protein databank; pNA, para-Nitroaniline; RMSD, Root mean square deviation; T2DM, Type 2 diabetes mellitus; THC, Δ^9 -tetrahydrocannabinol; VMD, Visual molecular dynamics; WHO, World Health Organisation.

* Corresponding author. Department of Biochemistry and Microbiology, Nelson Mandela University, P.O Box 77000, Port Elizabeth 6031, South Africa.

E-mail address: carminita.frost@mandela.ac.za (C.L. Frost).

<https://doi.org/10.1016/j.heliyon.2023.e23289>

Received 16 September 2023; Received in revised form 30 November 2023; Accepted 30 November 2023

Available online 6 December 2023

2405-8440/© 2023 The Authors. Published by Elsevier Ltd. This is an open access article under the CC BY-NC-ND license (<http://creativecommons.org/licenses/by-nc-nd/4.0/>).

1. Introduction

Diabetes mellitus (DM) is a chronic metabolic disease characterised by abnormal levels of glucose in the blood stream. According to the World Health Organisation (WHO), DM is the ninth leading cause of death, following a significant percentage (70 %) increase in cases since 2000 [1]. More than 500 million people (adults between 20 and 79 years of age) are living with DM worldwide and it is estimated that this number is likely to rise to 783 million by 2045 [2]. Uncontrolled DM can lead to a number of complications related to kidney damage, nerve damage, blindness and cardiovascular diseases [3–6]. Regulating glucose levels in the bloodstream is considered to be one of the first strategies for the management of DM, particularly type 2 diabetes mellitus (T2DM), which accounts for over 90 % of cases with DM. The management of T2DM can be achieved through several methods, which range from lifestyle modifications to pharmacotherapeutic approaches. Substantial research into the development of DM treatments has resulted in the identification of several molecular targets which allow for better control of glycaemic conditions [7]. Among these, dipeptidyl peptidase IV (DPP-IV) has gained increasing attention for its potential to regulate T2DM [8].

DPP-IV is a membrane-bound, serine protease ectoenzyme which is distributed in numerous tissues, including the intestine, vascular endothelium, the liver and pancreas [9]. Its most important catalytic function is the inactivation of incretin hormones, mainly glucose-dependent insulinotropic polypeptide hormone (GIP) and glucagon-like peptide 1 (GLP-1) [10]. GIP and GLP-1 are a group of gastrointestinal hormones released by the gut in response to food intake, which lowers blood glucose by stimulating insulin secretion, delaying gastric emptying, reducing glucagon concentrations and promoting pancreatic beta-cell proliferation [11,12]. However, incretins have been reported to have a short half-life (1–2 min) due to rapid degradation by DPP-IV [13]. Therefore, inhibition of DPP-IV might result in the prolongation of the half-life of incretins, which, in turn, increases beta-cell insulin secretion in the pancreas, thereby maintaining glucose homeostasis. Commercially available DPP-IV inhibitors include drugs such as linagliptin, vildagliptin, sitagliptin and saxagliptin, which act as reversible competitive inhibitors of the catalytic activity of this enzyme [9]. Current drugs are known to have a number of side effects, including pancreatitis, nasopharyngitis, hepatic disorders and gastrointestinal symptoms [14, 15]. Therefore, research efforts seeking alternative DPP-IV inhibitors that have fewer or no undesirable side effects have increased.

Plant-derived natural compounds have a long history of use in the treatment of various ailments [16]. The various phytoconstituents from medicinal plants are known for their therapeutic properties, structural diversity and low toxicity. These properties make them attractive for use in the development of novel anti-diabetic therapeutic agents. Hemp or *Cannabis sativa* L. (*C. sativa*) is one such plant that has been used for many years as a therapeutic agent against various ailments [17]. There are 3 species of *Cannabis* namely *Cannabis sativa*, *Cannabis indica* and *Cannabis ruderalis* belong to the family of Cannabaceae. Many traditional medicinal uses of *Cannabis* have been reported, particularly for the management of diabetes among different ethnic groups in India and South Africa [18–21]. It contains a wide range of phytochemicals which include cannabinoids, phenolic compounds and terpenes [22]. Among the various *C. sativa* phytochemicals, much attention has been primarily given to cannabinoids [22]. Out of many cannabinoids identified so far, Δ^9 -tetrahydrocannabinol (THC) is the most dominant, primarily responsible for the psychoactive effects of cannabis [23]. Other well-studied cannabinoids include cannabidiol (CBD), cannabinol (CBN), cannabigerol (CBG), cannabichromene (CBC), and cannabicyclol (CBL) [24]. Several studies have demonstrated that cannabinoids possess outstanding anti-diabetic properties, which include improving insulin sensitivity of tissues and protecting beta pancreatic cells from the destructive effects of hyperglycemia [25,26]. Furthermore, studies have demonstrated that CBD and THC may play a key role in DM treatment due to their ability to inhibit digestive enzymes relevant to T2DM [27,28].

Although there is increasing evidence suggesting that cannabinoids may be biologically active compounds contributing to the anti-diabetic properties, the potential inhibitory activity of cannabinoids against human DPP-IV and their mechanism of interaction with this enzyme remains unexplored. In this present study, we describe the evaluation of the selected cannabinoids' ability to inhibit recombinant human DPP-IV using *in vitro* assays. CBD, CBG, CBN, and THC were selected for this study because they are some of the most well-known and studied cannabinoids, and their standards are commercially available. Molecular docking on the active and allosteric site of DPP-IV was conducted to study the interactions between this enzyme and the selected cannabinoids. Molecular dynamics simulations were also performed to elucidate the dynamic behaviour of the interactions between DPP-IV and the cannabinoids.

2. Materials and methods

2.1. Materials

The commercial enzyme, recombinant human dipeptidyl peptidase IV, Gly-Pro-*p*-nitroanilide (CAS: 103213-34-9), commercially available inhibitor, sitagliptin (CAS: 654671-77-9) and buffer reagents were all purchased from Sigma Aldrich (St. Louis, United States of America). Cannabidiol (CBD), cannabigerol (CBG), cannabinol (CBN) and Δ^9 -tetrahydrocannabinol (THC) were purchased from Leco (St. Joseph, United States of America). All other reagents used were of an analytical grade.

2.2. Dipeptidyl peptidase IV inhibition assay

DPP-IV activity was assessed according to the modified procedure previously described [29]. The assay is based on the cleavage of chromogenic substrate Gly-Pro-*p*-nitroanilide (Gly-Pro-*p*NA) by DPP-IV to release *para*-nitroaniline (*p*NA) which is measured at 405 nm. The inhibitors tested were cannabinoids (CBD, CBG, CBN and THC) or sitagliptin (commercially available inhibitor). The enzyme was diluted with assay buffer (0.1 M Tris-HCl, pH 8). To each well of a 96-well plate, DPP-IV was added to a final enzyme solution of

0.05 U/mL. This was followed by the addition of cannabinoids (1–40 µg/mL) or sitagliptin (2–50 ng/mL), and the mixture was pre-incubated at 37 °C for 10 min to allow the inhibitor to interact with the enzyme. The reaction was initiated by the addition of substrate to a final concentration of 2 mM and the plate was incubated at 37 °C for 30 min. The total reaction volume in each well was 200 µL. The absorbance was measured at 405 nm every 2 min with a BioTek Epoch™ Microplate Spectrophotometer (Epoch Biotek Instruments, Winooski, United States of America). A control reaction mixture was prepared with all the above reagents, excluding the inhibitor (cannabinoids or sitagliptin) which was replaced with assay buffer (0.1 M Tris-HCl, pH 8). All assays were performed in triplicate and the average values were reported. The DPP-IV inhibitory effects of the cannabinoids were expressed as percentage inhibition, which was estimated as follows:

$$\% \text{ inhibition} = [(Abs_{\text{control}} - Abs_{\text{inhibitor}}) / Abs_{\text{control}}] \times 100$$

The concentration of inhibitor required to inhibit 50 % of enzyme activity under the assay conditions was defined as the IC₅₀ and was determined graphically using GraphPad Prism Software version 9.0 (GraphPad Inc., San Diego, United States of America).

2.3. Enzyme kinetic study

The DPP-IV enzymatic activity was determined in the absence and presence of cannabinoids at concentrations of 2.5, 5, 10 and 20 µg/mL, respectively. The enzyme activity was assayed using Gly-Pro-pNA at five concentrations, ranging from 0.25 to 2 mM, according to the method described in section 2.2. The data sets obtained from each enzyme assay were analysed using the nonlinear regression curve fit in GraphPad Prism Software version 9.0 to determine maximal velocity (V_{max}) and the Michaelis-Menten constant (K_M). For graphically identifying the type of enzyme inhibition, a Lineweaver-Burk plot was used.

2.4. Circular Dichroism analysis of enzyme-inhibitor interaction

Circular Dichroism (CD) analysis of secondary structural changes on DPP-IV was conducted using a Chirascan (Version 4.4.1) spectrometer (Applied Photophysics Ltd., Leatherhead, United Kingdom) equipped with a Peltier temperature controller with nitrogen gas at 20 °C. Spectra in the far-UV region (190–260 nm) were collected using a 0.1 cm path-length quartz cuvette (Hellma, Müllheim, Germany). Scans were taken for each sample (enzyme on its own or enzyme with inhibitors), the reference spectra of the respective media were subtracted, and the data averaged to reduce noise. The analysis was performed by the CONTIN program in the Dichroweb processing software [30]. The relative percentages of the secondary structural elements (α -helix, β -sheet, β -turn and unordered regions) in different DPP-IV samples were then determined.

2.5. Preparation of protein and ligands for docking studies

The three-dimensional (3D) structure of DPP-IV was retrieved from the Protein databank (PDB) with accession ID: 3BJM, resolution = 2.35 Å [31]. The 3D structure was prepared for molecular docking using Discovery Studio Visualizer (www.accelrys.com, v21.1.0.20298). This was completed by removing the co-crystallized ligand and water molecules. The chemical structure of CBD (CID: 644019), CBG (CID: 5315659), CBN (CID: 2543) and THC (CID: 16078) were retrieved from the PubChem database and saved in SybylMOL2 format using Discovery Studio Visualizer.

2.6. Molecular docking

Molecular docking was performed using AutoDock Vina [32]. All the molecular docking experiments were carried out on a computer cluster through the use of an open-source terminal emulator, PuTTY (<https://www.putty.org/>), with WinSCP (<https://winscp.net/eng/index.php>) for file transfer. The 3D structures of DPP-IV and cannabinoids were changed to pdbqt format. Docking parameters were derived from the co-crystallized ligand and they were as follows: center $x = 47.7$; center $y = 51.4$ and center $z = 37.4$; a large search area size $x = 80$; size $y = 80$ and size $z = 80$ was employed. The exhaustiveness parameter was set to 32 and the optimal pose was selected based on the ligand-protein best docking scores. After completing the docking process, nine probable docking structures were generated and the best combination was evaluated on the basis of docking score (kcal/mol), number of hydrogen bonds, and other weak interactions. Redocking of saxagliptin was performed to validate docking parameters and the interactions were compared to the X-ray co-crystal structure of saxagliptin complexed with DPP-IV. The docked complexes of the selected cannabinoids were then imported to Discovery Studio to visualise the potential interactions between the cannabinoids and DPP-IV binding site residues.

2.7. Molecular dynamics simulations

All molecular dynamics (MD) simulations were performed with GROMACS 2018.6 [33]. MD simulations were completed for the enzyme without a ligand and the enzyme in complex with ligand. The best configuration for the compound with the best binding was selected from molecular docking results and hydrogen atoms were added using Discovery studio. The topology of the ligand structure was created by CGENFF [34] using the force field CHARMM27. The enzyme and enzyme-ligand complexes were then centered in a cubic box, solvated with water and Na⁺ ions were added to neutralise the solvated system. The energy of the systems was minimised

via the steepest descent algorithm. This was followed by equilibration under the “isothermal-isobaric” conditions NVT (N = number of particles, V = volume, and T = temperature 300 K) and NPT (N = number of particles, P = pressure 1 bar, and T = temperature 300 K). This equilibrium process was carried out for 100 ps for each NVT and NPT system before the production run. Upon completion of the two equilibration processes, an MD production run was performed for 100 ns, at a temperature of 300 K, and pressure of 1 bar. Analysis was conducted by calculating various parameters on GROMACS 2018.6 and representing them as charts on GraphPad Prism 9.0 software. Visualisation of the simulations was performed on Visual molecular dynamics (VMD) [35]. One of the parameters that was calculated is the hydrogen bond distance between a residue and ligand at the binding site to determine the stability of the ligand. The root mean square deviation (RMSD) of ligand was calculated to determine how flexible a ligand is in the binding site. RMSD values of the enzyme (alone) and enzyme-ligand complexes were compared. Lastly, principal component analysis (PCA) of the enzyme (alone) and enzyme-ligand complexes was performed to study the movement of the protein during simulation.

2.8. Statistical analysis

All statistical analyses were performed using the data analysis feature in GraphPad Prism 9.0 software. Significant differences between compared data sets were determined by one-way analysis of variance (ANOVA). A p-value of less than 0.05 was considered to indicate statistically significant differences between compared data sets.

3. Results and discussion

3.1. Inhibitory effects of cannabinoids on dipeptidyl peptidase IV activity

Four cannabinoids, namely, CBD, CBG, CBN and THC were screened for their inhibitory potential against recombinant human DPP-IV using Gly-Pro-pNA as a substrate (Fig. 1A). Sitagliptin (2–50 ng/mL) was used as a positive control for the inhibition of this enzyme (Fig. 1B). The cannabinoids were evaluated at the concentration range of 1–40 $\mu\text{g/mL}$. All cannabinoids and sitagliptin exhibited a dose-dependent inhibition profile. The highest inhibition percentages for CBD, CBG, CBN and THC were 73.2 %, 81.1 %, 51.9 % and 21.6 % at 40 $\mu\text{g/mL}$, respectively. The ability of THC to inhibit DPP-IV was significantly lower than that of the other three cannabinoids. The modest inhibitory action of THC is very advantageous when taking into account the medicinal potential of cannabinoids. This is due to the fact that the primary psychoactive ingredient in cannabis is THC, whereas other cannabinoids like CBD have no intoxicating effects. Therefore, THC may be excluded when further evaluating the cannabinoids as therapeutic candidates for managing diabetes. Compared to the cannabinoids, sitagliptin showed significant inhibition at far lower concentrations. This was expected as sitagliptin is the currently used DPP-IV synthetic inhibitor approved in several countries. However, cannabinoids are more likely to be preferred because sustainable harvesting and cultivation of natural compounds can be more environmentally friendly, and *Cannabis* has a long history of human use.

The potency of cannabinoids as DPP-IV inhibitors was evaluated by determining their IC_{50} values (Table 1). The IC_{50} values of cannabinoids and sitagliptin were determined graphically by plotting the percentage inhibition of DPP-IV against the increasing concentration of the inhibitors. The IC_{50} determination was performed for those inhibitors which displayed more than 50 % in DPP-IV inhibition. The IC_{50} values were determined to be between 4.3 and 9.4 $\mu\text{g/mL}$ for CBD, 4.1–8.6 $\mu\text{g/mL}$ for CBG, 3.0–5.2 $\mu\text{g/mL}$ for CBN, and 6.3–9.8 ng/mL for sitagliptin. Although it is a commercially available DPP-IV inhibitor, sitagliptin is significantly potent. The selected cannabinoids are comparatively better inhibitors when compared to some previously reported plant-derived DPP-IV inhibitors. For example, it was reported that rutin from *Fagopyrum esculentum* was found to have an IC_{50} value of 296 $\mu\text{g/mL}$ against DPP-IV activity [36]. Other naturally available DPP-IV inhibitors such as cyanidin-3-glucoside, isoquercetin, lupeol and vitisin A were found to have IC_{50} values of 60.5, 44.9, 13.5 and 50.9 $\mu\text{g/mL}$, respectively [37–40]. Based on these findings, cannabinoids were found to be promising plant-derived DPP-IV inhibitory compounds.

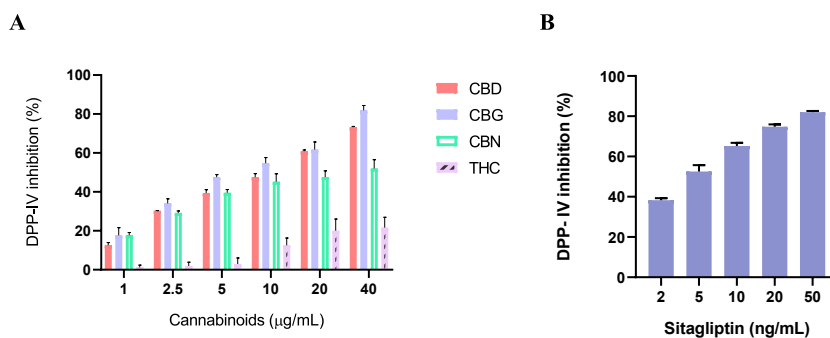


Fig. 1. Inhibitory effects of cannabinoids and sitagliptin (standard drug) on the activity of DPP-IV. Dose dependent inhibition of DPP-IV by (A) cannabinoids and (B) sitagliptin. Each datapoint represents the average \pm standard deviation of triplicate values.

Table 1
Determination of IC₅₀ values of inhibitors.

Inhibitor	IC ₅₀ value (μg/mL)
CBD	6.9 ± 0.85
CBG	6.4 ± 0.78
CBN	4.0 ± 0.29
Sitagliptin	0.0078 ± 0.0011

3.2. Determination of the mode of DPP-IV inhibition

A kinetic study was completed to investigate the type of inhibition displayed by cannabinoids. Fig. 2 illustrates the Lineweaver-Burk plots of each cannabinoid, and the kinetic parameters obtained from Michaelis-Menten non-linear regression analysis are displayed in Table 2. The kinetic analysis data suggested a mixed type of inhibition for the cannabinoids as the Lineweaver-Burk plots in the absence and presence of inhibitors intersected either above or below the negative x-axis (Fig. 2A–D). In terms of Michaelis constant (K_M) and maximal velocity (V_{max}), mixed inhibition is generally characterised by changes in K_M values which are accompanied by decreasing V_{max} values [41]. As shown in Table 2, cannabinoids followed this pattern as the V_{max} values are decreasing and there are changes in K_M values. Mixed inhibitors are reported to bind to both the free enzyme and the enzyme-substrate complex with varying degrees of affinity. An increase in K_M value is usually an indication that the inhibitor favours binding to the free enzyme, while a decreasing K_M value indicates that the inhibitor favours binding to the enzyme-substrate complex. The data from Table 2 indicated that K_M values for CBD and CBG were increasing, suggesting that these inhibitors might favour binding to the free enzyme. Fluctuating K_M values were observed for CBN and THC. This might be due to the modest inhibitory action exhibited by CBN and THC, as there was less change in the activity of the enzyme between inhibitor concentrations. Other plant-derived compounds such as hyperoside, narcissoside, cyanidin 3-O-glucoside, and isoliquiritigenin were also shown to inhibit DPP-IV in a mixed manner [42]. One advantage of mixed inhibitors is that they may not be affected by higher concentrations of the substrate. This implies that even at reduced concentrations, the inhibitor would still be effective.

3.3. Cannabinoid effects on DPP-IV secondary structure

To obtain further information regarding the nature of the interaction of DPP-IV with cannabinoids, CD analysis was performed. Detailed information about the secondary structure of the enzyme in the absence or presence of cannabinoids is presented in Fig. 3. The heat-inactivated enzyme was used as a positive control (red line). Sitagliptin (green line) was used as a control, as it is a known DPP-IV competitive inhibitor. In the absence of inhibitors (active DPP-IV), the CD spectra of the active enzyme showed a peak around the 225

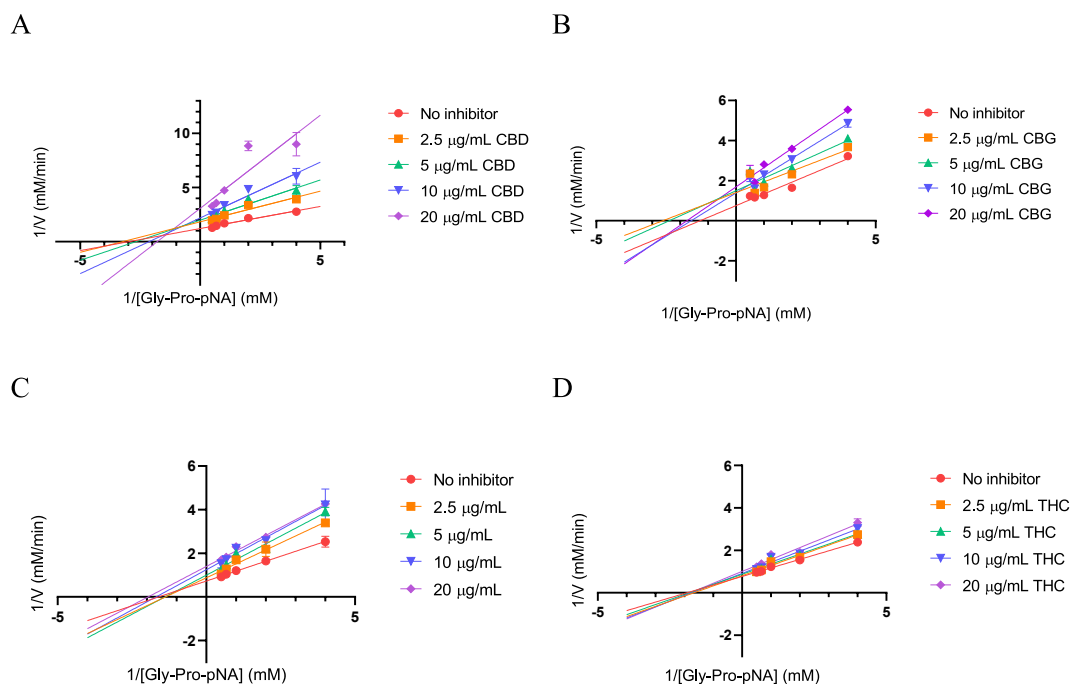


Fig. 2. Lineweaver-Burk plot of DPP-IV inhibition by cannabinoids. (A) CBD, (B) CBG, (C) CBN, and (D) THC. Each datapoint represents the average ± standard deviation of triplicate values.

Table 2
Kinetic parameters of DPP-IV in the absence/presence of inhibitors.

Kinetic parameter	Inhibitor concentration ($\mu\text{g/mL}$)	No inhibitor	CBD	CBG	CBN	THC
K_M (mM)		0.52				
	2.5		0.43	0.28	0.85	0.55
	5		0.58	0.33	0.63	0.59
	10		0.74	0.55	0.68	0.57
	20		1.3	0.56	0.5	0.56
V_{max} (mM/min)		1.2				
	2.5		0.61	0.68	1.01	1.1
	5		0.59	0.65	0.93	1.8
	10		0.55	0.70	0.86	1.0
	20		0.51	0.60	0.74	0.97

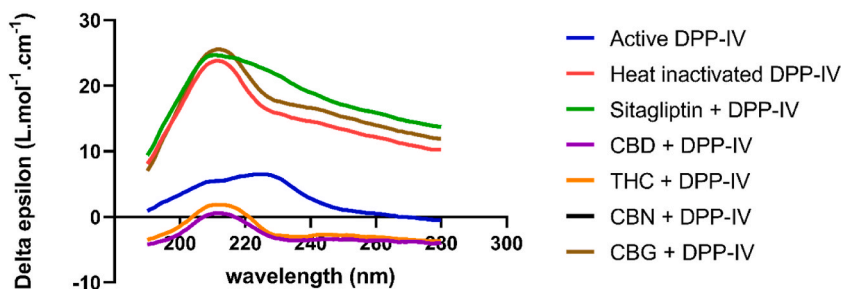


Fig. 3. Circular dichroism spectra showing secondary structural changes of DPP-IV upon interaction with inhibitors. Curves for CBD (purple) and CBN (black) were identical. Each data point represents the average \pm standard deviation of triplicate values. (For interpretation of the references to colour in this figure legend, the reader is referred to the Web version of this article.)

nm region. A shift in the peak towards the 208 nm region, upon the addition of inhibitors, was observed when compared to the CD spectra of the active enzyme. This pattern was quite prominent for the spectra of sitagliptin, CBG (brown line), and heat-inactivated enzyme (control). The CD spectra of CBD, CBN, and THC demonstrated a similar pattern. The two peaks in the region of 208 nm and 222 nm are attributed to the high α -helical content of the enzyme [43]. Furthermore, changes were observed in the deconvoluted proportions of β -sheets, α -helices, and unordered conformations (Table 3). Interaction of DPP-IV with the sitagliptin and CBG led to an increase in β -sheets and α -helix content and a decrease in unordered regions of the enzyme's secondary structure. In contrast, a decrease in β -sheets and α -helix content, and an increase in unordered regions was observed when the enzyme interacted with CBD, CBN, and THC. These findings suggest that the direct interaction of cannabinoids with DPP-IV is likely to lead to conformational changes in the secondary structure of the enzyme.

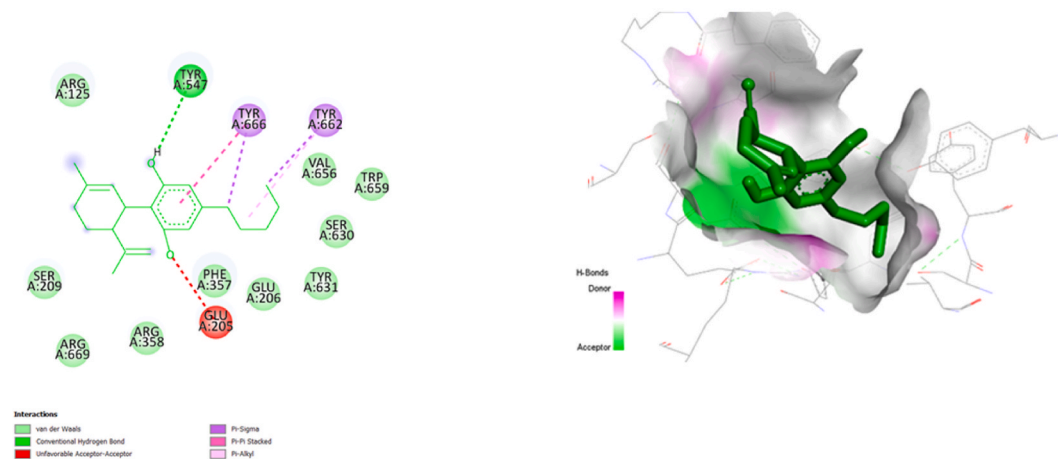
3.4. Molecular docking

In order to better understand the interactions between DPP-IV protein and cannabinoids, molecular docking studies were conducted. The X-ray structure used for docking studies was a recombinant human DPP-IV complexed with saxagliptin (resolution = 2.35 Å) [31]. Validation of docking parameters was carried out by redocking saxagliptin and the interactions are shown in the additional file1 (Fig. S1). The binding site and interacting residues matched those found in the X-ray co-crystal structure of saxagliptin complexed with DPP-IV, indicating that the parameters used in this study were valid. For the first set of docking experiments, cannabinoids were individually docked into the active site of the protein. Based on a molecular docking analysis, all four cannabinoids exhibited interactions with key amino acid residues in the active site (Fig. 4). It has been reported that DPP-IV has three binding pockets at the active site, namely S1, S2 and S3. The pockets S1 and S2 consist of Arg125, Ser209, Phe357, Arg358, Tyr547, Ser630, Ser631, Val656, Trp659, Tyr662, Tyr666, Asn710, Val711 and His740 [44,45]. Pocket S2 is the cavity located near Glu205, Glu206, and Tyr662. The

Table 3
The effects of cannabinoids and sitagliptin on the secondary structure of DPP-IV.

Inhibitor	α -helix %	β -sheets	β -turns	Unordered
Active enzyme	29.3	43.5	0.0	27.2
Heat inactivated	41.0	59.0	0.0	0.0
Sitagliptin	42.6	57.4	0.0	0.0
CBD	10.9	4.5	7.3	77.4
CBG	42.9	57.1	0.0	0.0
CBN	10.9	4.5	7.3	77.4
THC	10.0	4.4	8.3	77.3

A



B

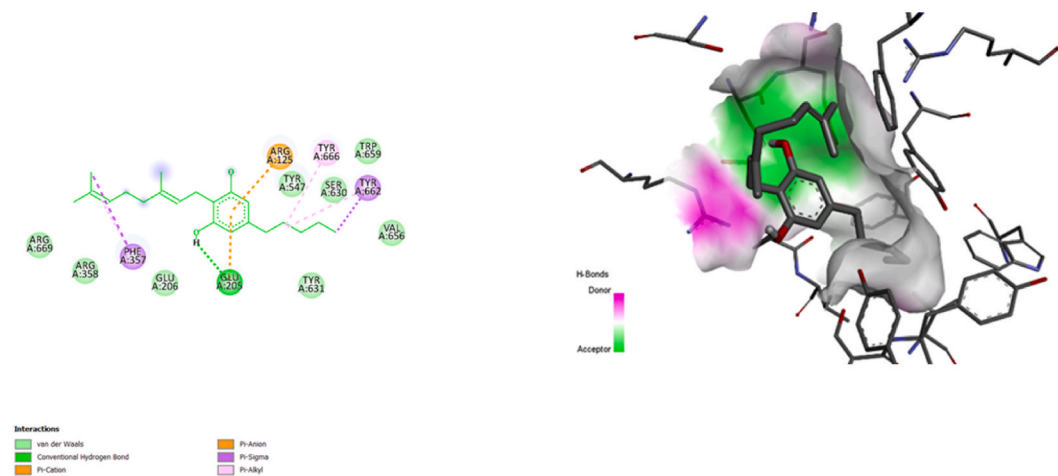


Fig. 4. Molecular docking analysis of the interaction of cannabinoids with DPP-IV. The analysis was performed for (A) CBD, (B) CBG, (C) CBN and (D) THC. On the left is the two-dimensional depiction, presenting the corresponding interacting amino acid residues within the binding site of DPP-IV (hydrogen bonds are represented by the dashed green lines). On the right, the detailed view of the docked cannabinoid structures and the potential of hydrogen bonding capacity within the binding site of DPP-IV is shown (purple presents the hydrogen bond donor region and green presents hydrogen bond acceptor region).. (For interpretation of the references to colour in this figure legend, the reader is referred to the Web version of this article.)

pocket S3 consists of Ser209, Arg358, and Phe357 [46]. From the docking analysis, it is clear that CBD interacted with the active site amino acid residues (Fig. 4A). CBD formed a van der Waals interaction network with amino acid residues from all three binding pockets. CBD also generated a hydrogen bond with residue Tyr547, which occupies pockets S1 and S2. Residues Tyr66 and Tyr662 were involved in P-sigma interactions with CBD. CBG generated a hydrogen bond with residue Glu205 (Fig. 4B). It has been reported that DPP-IV inhibitors form strong interactions with Glu205 and Glu206 by generating salt bridges with the glutamate residues [47]. CBG interacted with Glu205 through the formation of salt bridges and also generating a hydrogen bond, suggesting that this interaction is a combination of charge-charge and hydrogen bonding electrostatic interactions similar to what is found in the literature for other DPP-IV inhibitors. In the case of CBN (Fig. 4C), a hydrogen bond was generated with Glu206 and Pi-anion with Glu205. This was another case of a potential combination of charge-charge and hydrogen bonding electrostatic interactions. In addition, van der Waals interactions with several other amino acid residues from all three binding pockets, as well as additional Pi-sigma, Pi-anion, Pi-Pi-stacked and Pi-alkyl were involved in the interaction with CBN. The interaction for THC binding (Fig. 4D) was quite similar to that of CBD, suggesting a similar binding mechanism. THC generated a hydrogen bond with residue Tyr547 and a van der Waals interaction network with amino acid residues from all three binding pockets. Furthermore, P-sigma interactions with Tyr666 and Try662 were observed.

A summary of molecular docking findings is presented in Table 4. CBN generated the highest-ranking docking score at -8.2 kcal/

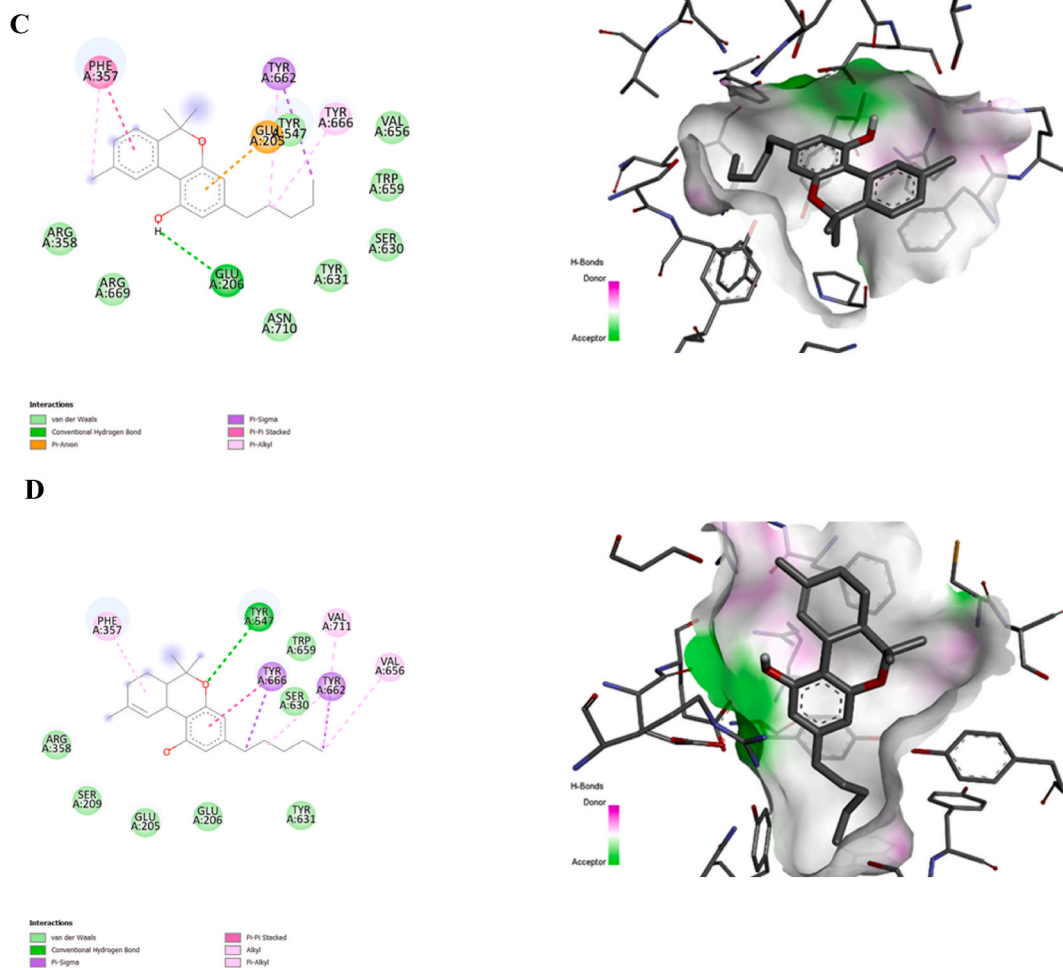


Fig. 4. (continued).

Table 4

Summary of molecular docking results of selected cannabinoids with the DPP-IV active site.

Compound	Docking score (kcal/mol)	Binding interactions	Interacting residues
CBD	-7.3	van der Waals, Hydrogen bonds, Pi-sigma, Pi-Pi stacked, Pi-alkyl	ARG125, GLU206, SER209, PHE357, ARG358, TYR546, SER630, TYP631, VAL656, TRP659, TYR662, TYR666
CBG	-6.5	van der Waals, Hydrogen bonds, Pi-sigma, Pi-cation, Pi-anion, Pi-alkyl	ARG125, GLU206, GLU205, PHE357, ARG358, SER630 TYR631, TYR547, VAL656, TYR659, TYR662, TYR666, ARG669
CBN	-8.2	van der Waals, Hydrogen bonds, Pi-sigma, Pi-anion, Pi-Pi stacked, Pi-alkyl	GLU206, GLU205, PHE357, ARG358, TYR547, SER630, TYR631, VAL656, TRP659, TYR662, TYR666, ARG669, ASN710
THC	-7.8	van der Waals, Hydrogen bonds, Pi-sigma, Pi-Pi stacked, Pi-alkyl, Alkyl	GLU205, GLU206, SER209, PHE357, ARG358, TYR547, VAL656, SER630, TYR631, TRP659, TYR662, TYR666, VAL711

mol, this was followed by THC at -7.8 kcal/mol, CBD at -7.3 kcal/mol and CBG at -6.5 kcal/mol. These findings reveal a possible correlation between the structure of the cannabinoids and their docking score. The two aromatic rings of CBN seem to be heavily involved in the interactions, suggesting a charge transfer attraction between its electron-rich aromatic rings and the positive charged groups of amino acid residues. Overall, all four cannabinoids are binding at the active site of DPP-IV by interacting with the key amino acid residues.

In addition to the binding information obtained from the active site, a second set of docking studies were performed to identify other potential sites that cannabinoids might bind to outside of the DPP-IV active site. This was carried out by increasing the docking area to include the entire structure of the protein (blind docking). The highest-ranking binding modes were then selected, and a summary of these findings is presented in Table 5. The docking scores of cannabinoids were comparable to the ones obtained from the

Table 5
Summary of molecular docking results of selected cannabinoids with DPP-IV allosteric site.

Compound	Docking score (kcal/mol)	Hydrogen bond	Binding interactions	Interacting residues
CBD	-7.3	ILE102	van der Waals, Hydrogen bonds, Pi-sigma, Pi-alkyl, Alkyl	GIY99, HIS100, ASN92, PHE95, LEU90, ASP96, ILE76, ILE102, ASN74
CBG	-6.5		van der Waals, Pi-Pi T shaped, Pi-alkyl, Alkyl	ASN562, PRO510, SER511, LYS512, PRO475, LEU514 ASP556, GLN527, PHE559, ALA564, ILE529, ARG560, VAL558
CBN	-8.0	ILE102	van der Waals, Hydrogen bonds, Pi-sigma, Pi-donor, Pi-alkyl, Alkyl	ASN74, ILE76, LEU90, GLU91, ASN92, PHE95, ASP96, ILE102, TYR105, LEU116,
THC	-8.0	PHE95	van der Waals, Hydrogen bonds, Pi-sigma, Pi-alkyl, Alkyl	LYS71, ASN74, ILE76, LEU90, GLU90, GLU91, ASN92, THR94, PHE95, ASP96, HIS100, ILE102,

active site docking. CBN and THC showed the highest docking score (-8.0 kcal/mol), followed by CBD at -7.3 kcal/mol and CBG remained at -6.5 kcal/mol. It should be noted that the amino acid residues identified at the binding sites have not yet been reported in the literature for their interaction with DPP-IV inhibitors. Therefore, it is highly possible that these two binding sites could be new allosteric binding sites. CBD, CBN and THC were binding at the same allosteric site and formed van der Waals, Pi-sigma, Pi-alkyl and alkyl interactions with Asn74, Lue90, Asn92, Phe95, Asp96 and His100. CBD and CBN generated a hydrogen bond with Ile102, and THC generated a hydrogen bond with Phe95. These interactions cooperate to form a stable DPP-IV-cannabinoid complex. The residues

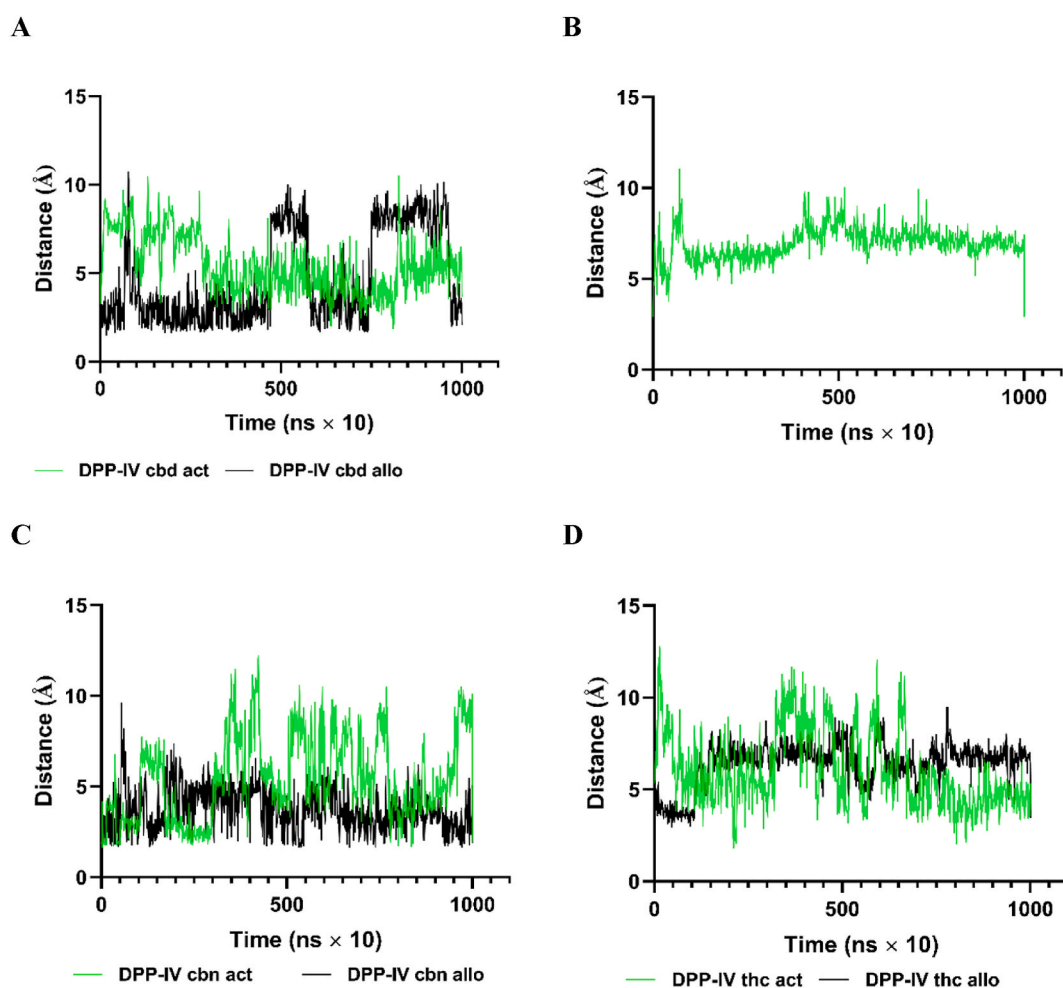


Fig. 5. Distance between cannabinoids and the binding site of DPP-IV during 100 ns MD simulation. For comparison, green represents the DPP-IV-cannabinoid complex at the active site and black represents the DPP-IV-cannabinoid complex at the allosteric site. The analysis was carried out with (A) CBD, (B) CBG, (C) CBN and (D) THC. The distance was calculated for the hydrogen bond that formed between cannabinoid and amino acid residue found in the binding site. (For interpretation of the references to colour in this figure legend, the reader is referred to the Web version of this article.)

that interacted with CBD, CBN, and THC have been reported to be part of the β chain region, which is involved in the movement of the exposure of the active site (45). On the other hand, CBG was bound to a different binding site, where it formed van der Waals, Pi-Pi T-shaped sigma, Pi-alkyl and alkyl interactions with Pro475, Pro510, Ser511, Lys512, Lue514, Phe559, and Val558. However, CBG showed far less potential to form a hydrogen bond, this might be attributed to the fact that most of the amino acid residues at this binding site are hydrophobic in nature. In terms of the structures, the cannabinoids with more than one ring exhibited strong docking scores towards the same allosteric binding site, while CBG, which possesses a single ring, preferred a more hydrophobic region. Overall, docking analysis revealed that cannabinoids are good binders and they fit well into the active and allosteric sites of the enzyme. Therefore, all four cannabinoids were selected for a further study to investigate the dynamic behaviour of the enzyme and

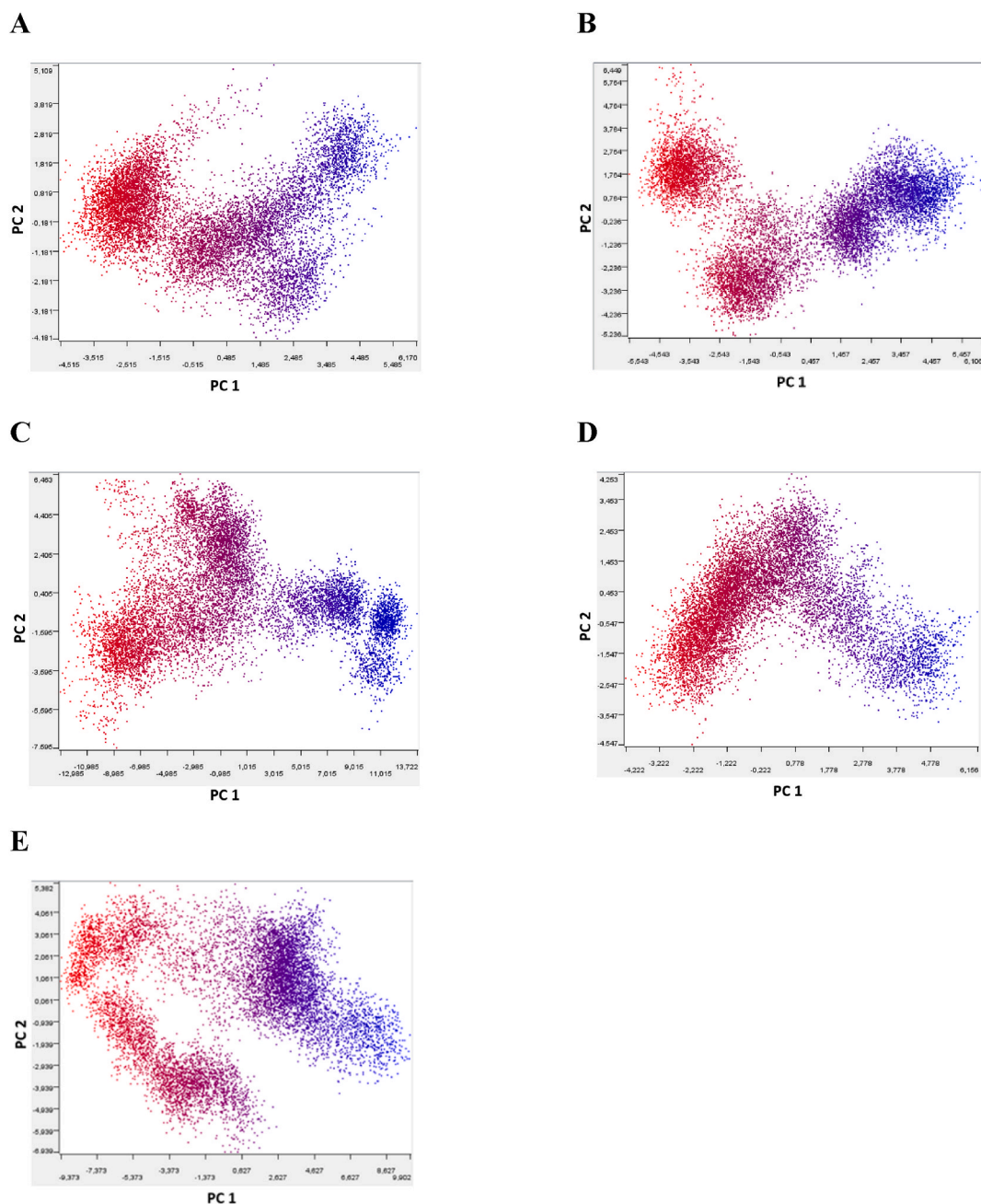


Fig. 6. Principal component analysis (PCA) for 100 MD simulation. (A) PCA for DPP-IV alone, (B) CBD at the allosteric site, (C) CBG at the active site, (D) CBN at the allosteric site, and (E) THC at the allosteric site. The trajectories generated by 100 ns MD simulations are colour-coded from red to blue (red = start and blue = end). (For interpretation of the references to colour in this figure legend, the reader is referred to the Web version of this article.)

ligand complexes.

3.5. Molecular dynamics simulations

Molecular docking approaches can be useful in identifying the interaction between a ligand (inhibitor) and a target protein. Docking studies allow a good estimation if a ligand fits well into a particular site of a target protein and this gives an indication if the ligand is a good binder. However, molecular docking can be limited as it provides only static interactions of protein and ligands. To better understand the differences between excellent and poor binders, analysis of conformational rearrangements of protein and ligand should be performed [48]. The 100 ns MD simulation of enzyme-ligand complex was performed by using GROMACS software in order to gain a deeper understanding of the stability and interactions of DPP-IV and cannabinoid complexes. Simulation of the enzyme without ligand was also conducted under identical conditions, to compare with enzyme-ligand complex. During molecular docking, it was found that cannabinoids had good docking scores for both active and allosteric site binding. However, it is possible that only weak interactions between the ligand and the binding site exist. To determine if any of the cannabinoids remain bound at the active or allosteric site under dynamic force, the hydrogen bond distance between a particular cannabinoid and selected residue was calculated (Fig. 5). The green line represents a hydrogen bond at the active site, while the black line represents a hydrogen bond at the allosteric site. CBG (Fig. 5B) didn't form hydrogen bonds at the allosteric site and the analysis was conducted with only the information obtained from the active site. It is clear that CBG remained attached to the active site throughout the 100 ns DM simulation without any significant fluctuations in hydrogen bond distance. These results suggest that CBG interacts with DPP-IV by binding at the active site and is likely to favour binding to the free enzyme. In the case of CBD (Fig. 5A), binding at the allosteric site remained stable for almost half the MD simulation time and thereafter, a few sharp fluctuations in bond distance were observed, but the ligand re-entered the binding site towards the end of simulation. The binding at the active site resulted in a number of sharp fluctuations, which were more frequent and remained throughout the 100 ns MD simulation. This dynamic behaviour was more pronounced for CBN (Fig. 5C) and THC (Fig. 5D), where these ligands remained bound to the allosteric site compared to the active site. Thus, it could be inferred that CBD,

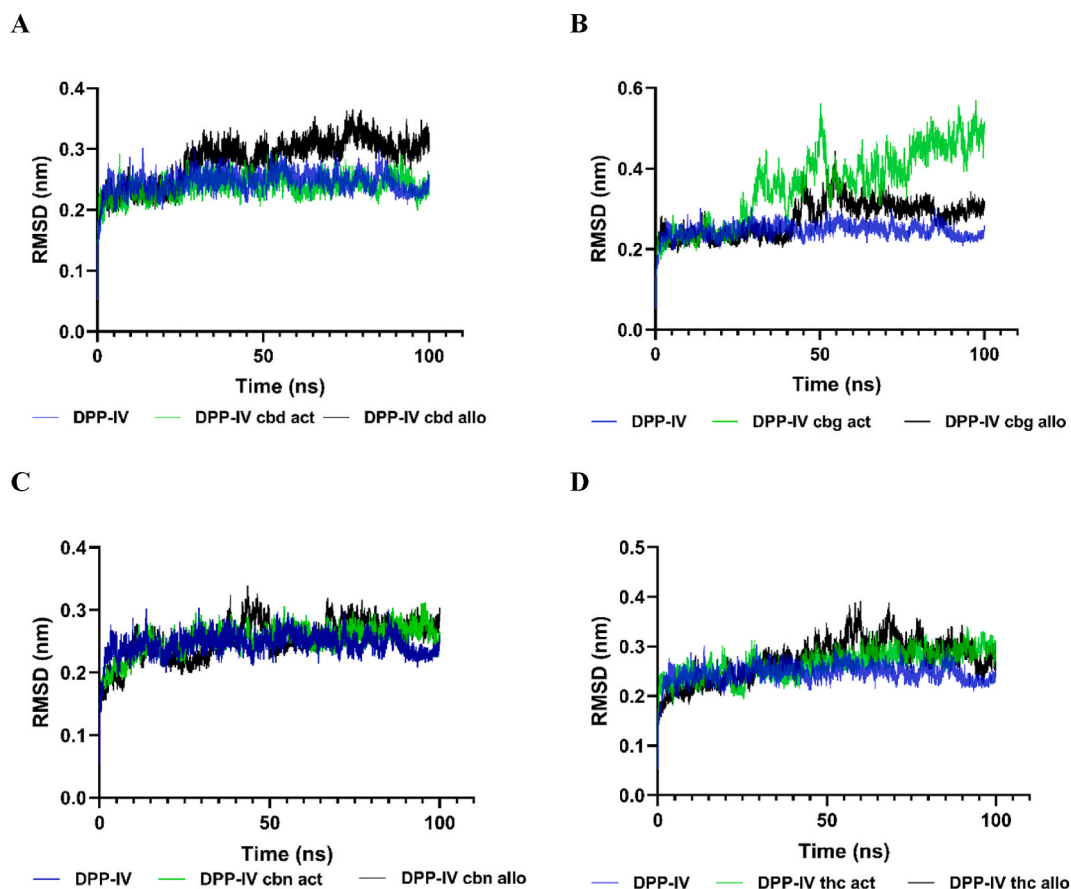


Fig. 7. Root mean square deviation (RMSD) values of the DPP-IV and DPP-IV-cannabinoid complexes. Analysis was performed for (A) CBD, (B) CBG, (C) CBN and (D) THC. Blue represents RMSD values for DPP-IV alone, green represents RMSD values for DPP-IV-cannabinoid complex at the active site and black represents RMSD values for the DPP-IV-cannabinoid complex at the allosteric site. (For interpretation of the references to colour in this figure legend, the reader is referred to the Web version of this article.)

CBN and THC inhibit DPP-IV by binding to the allosteric site, whereas CBG is likely to be an active site inhibitor. These findings support the enzyme kinetic analysis, which showed that cannabinoids are mixed DPP-IV inhibitors. Mixed inhibitors are likely not to be affected by higher substrate concentrations as they do not compete with the substrate.

3.5.1. Principal component analysis

The abovementioned results on the hydrogen bond distance provided an indication of whether the ligands remained bound to the binding site under dynamic force. However, the results didn't reveal whether the binding of the ligand induced conformational changes to the structure of the enzyme, thereby influencing its activity. To determine if the binding affects the enzyme dynamics, PCA was used to analyse the dynamics of the enzyme alone and the enzyme-cannabinoid complexes. Two eigenvector projections (PC1 and PC2) for DPP-IV and DPP-IV and cannabinoid complexes are shown in Fig. 6. PCA is an effective and useful technique to simplify complicated movements of long trajectories generated by MD simulations [49,50]. The graph indicates the variance in the conformational distribution, where each dot represents one conformation of the complex. The continuous colour representation (from red to blue) highlights the periodic jumps between these conformations. On comparing the collective motions of the DPP-IV and protein-cannabinoid complexes, clear differences were observed in collective motions due to binding of the cannabinoids. DPP-IV alone (Fig. 6A) displayed conformational space with a motional change between -4.515 and $+6.170$ in the PC1 axis and -4.181 to $+5.109$ in the PC2 axis. DPP-IV-CBD complex (Fig. 6B) exhibited three well-defined clusters with motional changes between -5.243 and $+6.106$ in the PC1 axis and -5.236 and $+6.449$ in the PC2 axis. In the case of the DPP-IV-CBG complex (Fig. 6C), a larger conformational space was observed, showing changes between -12.985 and $+13.722$ in the PC1 axis and -7.595 and $+6.463$ in the PC2 axis. The DPP-IV-CBN complex (Fig. 6D) showed lesser conformational space and two mixed large clusters with a motion between -4.222 and $+6.156$ in the PC1 axis and -4.547 and $+4.253$ in the PC2 axis. DPP-IV-THC (Fig. 6E) displayed motional changes between -9.373 and $+9.902$ in the PC1 axis and -6.939 and $+5.383$ in the PC2 axis. PCA could effectively demonstrate that binding of cannabinoids affects the enzyme dynamics differently. The data suggests that the free enzyme and the ligand-bound complex have conformational differences. Therefore, the ligands remained bound to the binding site under dynamic force as shown in Fig. 5, and induced conformational changes to the structure of the enzyme. This is in agreement with the findings obtained from CD analysis (Fig. 3) where it was demonstrated that the interaction of cannabinoids with DPP-IV leads to conformational changes in the secondary structure of the enzyme. Thus, it can be speculated that the binding of the cannabinoids results in conformational changes in the structure of the enzyme, in turn, influences the catalytic function of the enzyme.

3.5.2. Root mean square deviation analysis

To gain insight into the conformational stability of the enzyme structure during the 100 ns MD simulation, the structural changes and dynamic behaviour of enzyme-ligand complex were analysed through RMSD. The stability of DPP-IV-cannabinoid complexes were investigated by comparing the RMSD values of enzyme-ligand complex with the corresponding values of enzyme without the ligand in respect of their backbone. RMSD analysis measures the average distance between the selected atoms of superimposed protein, indicating the closeness between 3D structures [51,52]. Fig. 7 displays the enzyme RMSD trajectories for DPP-IV alone (blue), DPP-IV-cannabinoid complexes at the active (green) and allosteric sites (black). A complex is generally considered to have reached a stable state if the fluctuations in RMSD values are within 0.1 nm [53]. In the case of the DPP-IV-CBD complex (Fig. 7A), RMSD values depicted a stable configuration except for a slight deviation around 25 ns for allosteric site binding (black line) followed by stabilisation. The DPP-IV-CBD complex for active site binding (Fig. 7B) was stable until 25 ns–55 ns, before it started fluctuating until it reached equilibrium again at 75 ns. RMSD analysis revealed that the DPP-IV-CBN complex (Fig. 7C) and the DPP-IV-THC complex (Fig. 7D) remained stable throughout the 100 ns MD simulation without any significant variance. These findings showed that the DPP-IV-cannabinoid complexes remained relatively stable during MD simulation.

In order to better understand the ligand stability within the enzyme binding site during the 100 ns MD simulation, the RMSD values of the ligands were also evaluated (Fig. 8). Measurement of the RMSD values of the ligands would provide important information regarding the orientation of simulated cannabinoids with respect to their binding sites. Smaller RMSD variations show the stability of the ligand binding. As shown in Fig. 8A, CBD showed good binding stability with its RMSD values fluctuating gently around a low level (less than 0.1 nm). This was more prominent for the binding corresponding to the allosteric site. In the case of CBG (Fig. 8B), slight fluctuations from the start to 25 ns were observed, but the system reached stability for the entire MD simulation. For CBN in the DPP-IV-CBN complex (Fig. 8C) at the allosteric site (black), fluctuations can be seen from the beginning to 12 ns and these remained stable up to 45 ns; fluctuations occurred again between 45 ns and 55 ns and the ligand remained stable until the end of 100 ns simulation. Finally, RMSD values for THC (Fig. 8D) fluctuated within the 0.1 nm limit for the most part, indicating that the binding was stable during the 100 ns MD simulation. Overall, these results suggest that the structures of cannabinoids were stable after interaction with human DPP-IV. The results suggested that the residues at the binding sites on interaction with the cannabinoids displayed stability in the overall run. Therefore, the inhibitory activity displayed by cannabinoids is likely to be due to these interactions.

The study demonstrated the potent inhibitory potential of the selected cannabinoids against DPP-IV activity, a well-known T2DM therapeutic target. This is preliminary evidence for the potential application of the selected cannabinoids in maintaining glucose homeostasis, suggesting that they could be suitable therapeutic candidates for managing T2DM. To date, no study has focused on the inhibition of DPP-IV by cannabinoids, to our knowledge, our study is the first of its kind on this subject. However, further research including *in vivo* studies will be interesting to explore the ability of cannabinoids to inhibit DPP-IV *in vivo* or enhance the plasma concentrations of incretin hormones, particularly GLP-1 and GIP. The *in vitro* and *in silico* data from this study are still significant since they offer some indication of the selected cannabinoids' potential as DPP-IV inhibitors, which may serve as the foundation for further research *in vivo*.

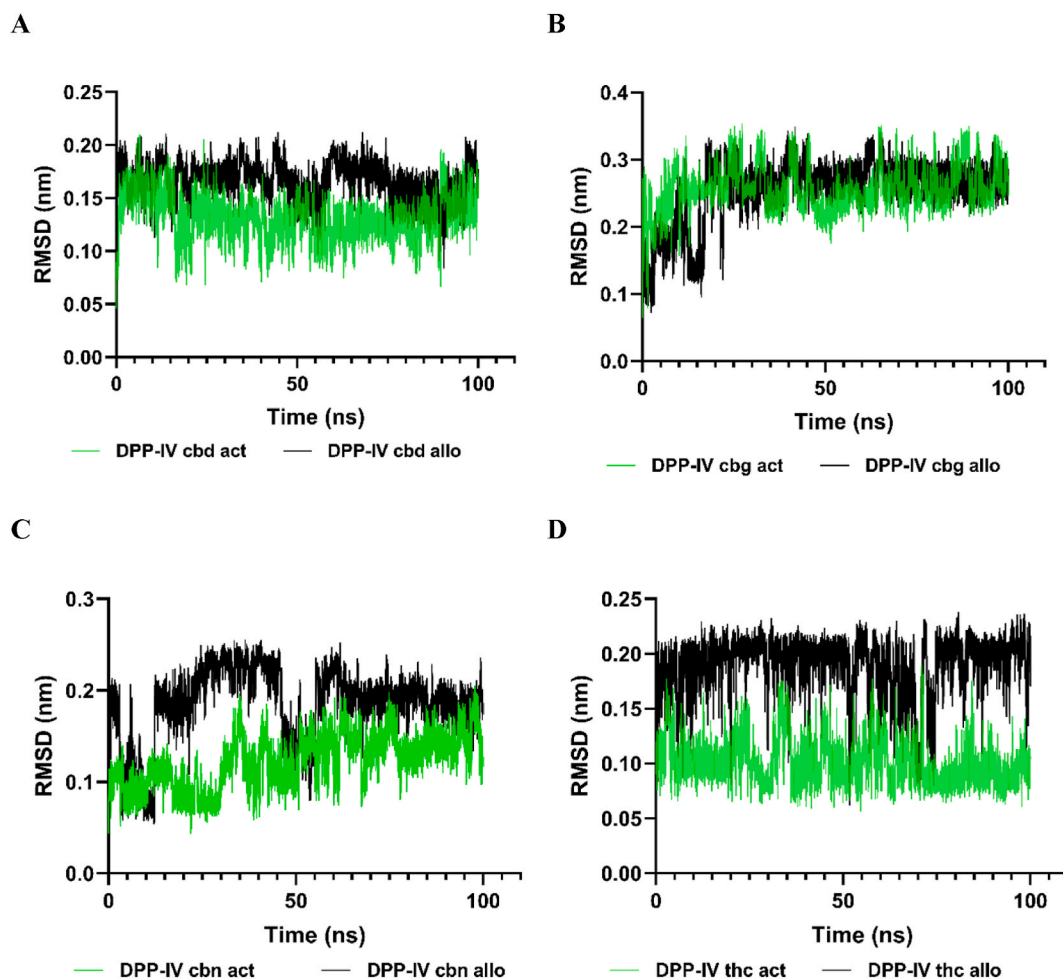


Fig. 8. Root mean square deviation (RMSD) values of cannabinoids in the DPP-IV-cannabinoid complex. Green represents RMSD values for the DPP-IV-cannabinoid complex at the active site and black represents RMSD values for the DPP-IV-cannabinoid complex at the allosteric site. RMSD values shown are for (A) CBD, (B) CBG, (C) CBN and (D) THC. (For interpretation of the references to colour in this figure legend, the reader is referred to the Web version of this article.)

4. Conclusion

Human DPP-IV is a key enzyme in the catalytic degradation of incretin hormones. Inhibition of this enzyme can lead to improved insulin secretion, which in turn helps in maintaining glucose homeostasis. The data from the current study has established the *in vitro* DPP-IV inhibitory activity of the selected cannabinoids. CBG resulted in the highest inhibitory activity (81.1 %), while THC showed less inhibitory potential, yielding only 21.6 % inhibition at 40 $\mu\text{g}/\text{ml}$ concentration. The mechanism of enzyme inhibition for all four tested cannabinoids was identified as mixed type inhibition and the data suggested that CBD and CBG may favour binding to the free enzyme. CD spectra data further confirmed that interactions between cannabinoids and enzyme resulted in changes in the secondary structural elements of the enzyme, suggesting a direct interaction. Molecular docking and molecular dynamics simulation studies were performed in order to further elucidate the interactions between cannabinoids and DPP-IV. Molecular docking studies revealed that cannabinoids could bind well to the active and allosteric sites with comparable docking scores. However, molecular dynamics simulation studies indicated that under dynamic force, CBD, CBN and THC were more likely to remain bound at the allosteric site, while CBG preferred binding at the active site. Cannabinoids were also shown to be highly stable and compact in forming complexes with DPP-IV, as evidenced by the 100 ns molecular dynamics simulation runs. This knowledge regarding the mechanisms of inhibition could lead to improved applications of these selected cannabinoids as DPP-IV inhibitors. Overall, this study suggests that cannabinoids possess the benefits of plant-derived inhibitors against DPP-IV, which is promising for the management of hyperglycemia.

Data availability statement

Data will be made available on request and is not published in a public repository.

Additional information

Additional file1.

CRedit authorship contribution statement

Lithalethu Mkabayi: Writing – original draft, Methodology, Formal analysis, Conceptualization. **Zenobia Viljoen:** Formal analysis, Data curation, Conceptualization. **Rui W.M. Krause:** Supervision, Methodology, Formal analysis, Conceptualization. **Kevin A. Lobb:** Writing – review & editing, Supervision, Methodology, Formal analysis, Conceptualization. **Brett I. Pletschke:** Writing – review & editing, Supervision, Funding acquisition, Conceptualization. **Carminita L. Frost:** Writing – review & editing, Supervision, Methodology, Funding acquisition, Conceptualization.

Declaration of competing interest

The authors declare that they have no known competing financial interests or personal relationships that could have appeared to influence the work reported in this paper.

Acknowledgements

We would acknowledge Rhodes University, Nelson Mandela University (NMU) and the National Research Foundation (NRF), South Africa for their financial support during this study. We wish to thank the reviewers for their critical feedback.

Appendix A. Supplementary data

Supplementary data to this article can be found online at <https://doi.org/10.1016/j.heliyon.2023.e23289>.

References

- [1] WHO, The Top 10 Causes of Death, 2020. Available online: <https://www.who.int/news-room/fact-sheets/detail/the-top-10-causes-of-death>. (Accessed 18 January 2023).
- [2] International Diabetes Federation, The IDF Diabetes Atlas, tenth ed., 2021.
- [3] K. Stadler, V. Jenei, A. Somogyi, J. Jakus, Beneficial effects of aminoguanidine on the cardiovascular system of diabetic rats, *Diabetes-Metab. Res.* 21 (2005) 189.
- [4] S. Roy, T.S. Kern, B. Song, C. Stuebe, Mechanistic insights into pathological changes in the diabetic retina: implications for targeting diabetic retinopathy, *Am. J. Pathol.* 187 (2017) 9.
- [5] J. Lu, Y. Luo, J. Wang, C. Hu, R. Zhang, Association of type 2 diabetes susceptibility loci with peripheral nerve function in a Chinese population with diabetes, *J. Diabetes Investig.* 8 (2017) 115–120.
- [6] U. Galicia-Garcia, A. Benito-Vicente, S. Jebari, A. Larrea-Sebal, H. Siddiqi, K.B. Uribe, H. Ostolaza, C. Martin, Pathophysiology of type 2 diabetes mellitus, *Int. J. Mol. Sci.* 21 (2020) 6275.
- [7] A. Kanwal, N. Kanwar, S. Bharati, P. Srivastava, S.P. Singh, S. Amar, Exploring new drug targets for type 2 diabetes: success, challenges and opportunities, *Biomedicines* 10 (2) (2022) 331.
- [8] S. Chhabria, S. Mathur, S. Vadakan, D.K. Sahoo, P. Mishra, B. Paital, A review on phytochemical and pharmacological facets of tropical ethnomedicinal plants as reformed DPP-IV inhibitors to regulate incretin activity, *Front. Endocrinol.* 13 (2022).
- [9] C.F. Deacon, Physiology and pharmacology of DPP-4 in glucose homeostasis and the treatment of type 2 diabetes, *Front. Endocrinol.* 10 (2019) 80.
- [10] A.K. Singh, Dipeptidyl peptidase-4 inhibitors: novel mechanism of actions, *Indian J. Endocrinol. Metab.* 18 (6) (2014) 753.
- [11] J.E. Campbell, D.J. Drucker, Pharmacology, physiology, and mechanisms of incretin hormone action, *Cell Metabol.* 17 (6) (2013) 819–837.
- [12] S. Chatterjee, K. Khunti, M.J. Davies, Type 2 diabetes, *Lancet* 389 (2017) 2239–2251.
- [13] A. Capuano, L. Sportiello, M.I. Maiorino, F. Rossi, D. Giugliano, K. Esposito, Dipeptidyl peptidase-4 inhibitors in type 2 diabetes therapy—focus on alogliptin, *Drug Des. Dev. Ther.* 7 (2013) 989.
- [14] P. Aschner, M.S. Kipnes, J.K. Lunceford, M. Sanchez, C. Mickel, D.E. Williams-Herman, Sitagliptin Study 021 Group, Effect of the dipeptidyl peptidase-4 inhibitor sitagliptin as monotherapy on glycemic control in patients with type 2 diabetes, *Diabetes Care* 29 (12) (2006) 2632–2637.
- [15] L. Jones, A.M. Jones, Suspected adverse drug reactions of the type 2 antidiabetic drug class dipeptidyl-peptidase IV inhibitors (DPP4i): can polypharmacology help explain? *Pharmacol. Res. Perspect.* 10 (6) (2022), e01029.
- [16] L.D. Kapoor, *Handbook of Ayurvedic Medicinal Plants: Herbal Reference Library*, Routledge, Newyork, 2017.
- [17] P.B. Sampson, Phytocannabinoid pharmacology: medicinal properties of *cannabis sativa* constituents aside from the “Big Two”, *J. Nat. Prod.* 84 (1) (2020) 142–160.
- [18] D.R. Chhetri, P. Parajuli, G.C. Subba, Antidiabetic plants used by Sikkim and Darjeeling Himalayan tribes, India, *J. Ethnopharmacol.* 99 (2) (2005) 199–202.
- [19] S.S. Semenya, A. Maroyi, A review of plants used against diabetes mellitus by Bapedi and Vhavenda ethnic groups in the Limpopo Province, South Africa, *Asian J. Pharmaceut. Clin. Res.* 12 (10) (2019) 44–50.
- [20] E. Frimpong, M. Nlooto, Management of diabetes and hypertension among Tswana and Zulu traditional health practitioners: a comparative cross-sectional study using a mixed-methods approach, *Afr. J. Biomed. Res.* 23 (2) (2020) 135–146.
- [21] I.E. Cock, N. Ndlovu, S.F. Van Vuuren, The use of South African botanical species for the control of blood sugar, *J. Ethnopharmacol.* 264 (2021), 113234.
- [22] C.M. Andre, J.F. Hausman, G. Guerriero, *Cannabis sativa*: the plant of the thousand and one molecules, *Front. Plant Sci.* 7 (2016) 19.
- [23] P.F. Whiting, R.F. Wolff, S. Deshpande, M. Di Nisio, S. Duffy, A.V. Hernandez, et al., Cannabinoids for medical use: a systematic review and meta-analysis, *JAMA* 313 (24) (2015) 2456–2473.
- [24] M. ElSohly, W. Gul, Constituents of *Cannabis sativa*, in: R.G. Pertwee (Ed.), *Handbook of Cannabis*, Oxford University Press, Oxford, 2014, pp. 3–22.
- [25] R.A. Levendal, D. Schumann, M. Donath, C.L. Frost, Cannabis exposure associated with weight reduction and β -cell protection in an obese rat model, *Phytomedicine* 19 (7) (2012) 575–582.

- [26] S. Ramlugon, R.A. Levendal, C.L. Frost, Time-dependent effect of phytocannabinoid treatments in fat cells, *Phytother Res.* 32 (6) (2018) 1080–1089.
- [27] H. Ma, H. Li, C. Liu, N.P. Seeram, Evaluation of cannabidiol's inhibitory effect on alpha-glucosidase and its stability in simulated gastric and intestinal fluids, *J. Cannabis Res.* 3 (1) (2021) 1–6.
- [28] W. Suttithumsatid, M.A. Shah, S. Bibi, P. Panichayupakaranant, α -Glucosidase inhibitory activity of cannabidiol, tetrahydrocannabinol and standardized cannabinoid extracts from *Cannabis sativa*, *Curr. Res. Food Sci.* 5 (2022) 1091–1097.
- [29] P.S. Unnikrishnan, K. Suthindhiran, M.A. Jayasri, Antidiabetic potential of marine algae by inhibiting key metabolic enzymes, *Front. Life Sci.* 8 (2) (2015) 148–159.
- [30] N. Sreeram, R.W. Woody, Estimation of protein secondary structure from circular dichroism spectra: comparison of CONTIN, SELCON, and CDSSTR methods with an expanded reference set, *Anal. Biochem.* 287 (2000) 252–260.
- [31] W.J. Metzler, J. Yanchunas, C. Weigelt, K. Kish, H.E. Klei, D. Xie, Y. Zhang, M. Corbett, J.K. Tamura, B. He, L.G.M.S. Hamann, Kirby, J. Marcinkeviciene, Involvement of DPP-IV catalytic residues in enzyme-saxagliptin complex formation, *Protein Sci.* 17 (2008) 240–250.
- [32] O. Trott, A.J. Olson, AutoDock Vina, Improving the speed and accuracy of docking with a new scoring function, efficient optimization, and multithreading, *J. Comput. Chem.* 31 (2010) 455–461.
- [33] M.J. Abraham, T. Murtola, R. Schulz, S. Páll, J.C. Smith, B. Hess, E. Lindahl, GROMACS: high-performance molecular simulations through multi-level parallelism from laptops to supercomputers, *SoftwareX* 1 (2015) 19–25.
- [34] K. Vanommeslaeghe, E. Hatcher, C. Acharya, S. Kundu, S. Zhong, J. Shim, E. Darian, O. Guvench, P. Lopes, I. Vorobyov, A.D. Mackerell Jr., CHARMM general force field: a force field for drug-like molecules compatible with the CHARMM all-atom additive biological force fields, *J. Comput. Chem.* 31 (2010) 671–690.
- [35] W. Humphrey, A. Dalke, K. Schulten, VMD: visual molecular dynamics, *J. Mol. Graph. Model.* 14 (1996) 33–38.
- [36] A. Gupta, G.A. Jacobson, J.R. Burgess, H.F. Jelinek, D.S. Nichols, C.K. Narkowicz, H.A. Al-Aubaidy, Citrus bioflavonoids dipeptidyl peptidase-4 inhibition compared with gliptin antidiabetic medications, *Biochem. Biophys. Res. Commun.* 503 (2018) 21–25.
- [37] G. Cásedas, F. Les, E. González-Burgos, M.P. Gómez-Serranillos, C. Smith, V. López, Cyanidin-3-O-glucoside inhibits different enzymes involved in central nervous system pathologies and type-2 diabetes, *South Afr. J. Bot.* 120 (2019) 241–246.
- [38] L. Zhang, S.T. Zhang, Y.C. Yin, S. Xing, W.N. Li, X.Q. Fu, Hypoglycemic effect and mechanism of isoquercitrin as an inhibitor of dipeptidyl peptidase-4 in type 2 diabetic mice, *RSC Adv.* 8 (2018) 14967–14974.
- [39] S. Saleem, L. Jafri, I. ul Haq, L.C. Chang, D. Calderwood, B.D. Green, B. Mirza, Plants *Fagonia cretica* L. and *Hedera nepalensis* K. Koch contain natural compounds with potent dipeptidyl peptidase-4 (DPP-4) inhibitory activity, *J. Ethnopharmacol.* 156 (2014) 26–32.
- [40] Y.S. Lin, C.R. Chen, W.H. Wu, C.L. Wen, C.I. Chang, W.C. Hou, Anti- α -glucosidase and anti-dipeptidyl peptidase-IV activities of extracts and purified compounds from *Vitis thunbergii* var. *taiwaniana*, *J. Agric. Food Chem.* 63 (2015) 6393–6401.
- [41] A.A. Saboury, Enzyme inhibition and activation: a general theory, *J. Iran. Chem. Soc.* 6 (2009) 219–229.
- [42] J. Pan, Q. Zhang, C. Zhang, W. Yang, H. Liu, Z. Lv, J. Liu, Z. Jiao, Inhibition of dipeptidyl peptidase-4 by flavonoids: structure–activity relationship, kinetics and interaction mechanism, *Front. Nutr.* 9 (2022).
- [43] P.K. Kempegowda, F. Zameer, S.K. Murari, Delineating antidiabetic proficiency of catechin from *Withania somnifera* and its inhibitory action on dipeptidyl peptidase-4 (DPP-4), *Biomed. Res.* 29 (2018) 3192–3200.
- [44] B.R. Kim, H.Y. Kim, I. Choi, J.B. Kim, C.H. Jin, A.R. Han, DPP-IV inhibitory potentials of flavonol glycosides isolated from the seeds of *Lens culinaris*: *in vitro* and molecular docking analyses, *Molecules* 23 (8) (2018) 1998.
- [45] S.Q. Pantaleão, E.A. Philot, P.T. de Resende-Lara, A.N. Lima, D. Perahia, M.A. Miteva, et al., Structural dynamics of DPP-4 and its influence on the projection of bioactive ligands, *Molecules* 23 (2) (2018) 490.
- [46] J. Fan, M.H. Johnson, M.A. Lila, G. Yousef, E.G. De Mejia, Berry and citrus phenolic compounds inhibit dipeptidyl peptidase IV: implications in diabetes management, *Evid.-Based Complementary Altern. Med.* 2013 (2013).
- [47] S. Arulmozhiraja, N. Matsuo, E. Ishitsubo, S. Okazaki, H. Shimano, H. Tokiwa, Comparative binding analysis of dipeptidyl peptidase IV (DPP-4) with antidiabetic drugs—an *ab initio* fragment molecular orbital study, *PLoS One* 11 (11) (2016), e0166275.
- [48] V. Salmasso, S. Moro, Bridging molecular docking to molecular dynamics in exploring ligand-protein recognition process: an overview, *Front. Pharmacol.* 9 (2018) 923.
- [49] A. Wolf, K.N. Kirschner, Principal component and clustering analysis on molecular dynamics data of the ribosomal L11·23S subdomain, *J. Mol. Model.* 19 (2013) 539–549.
- [50] C.C. David, D.J. Jacobs, Principal component analysis: a method for determining the essential dynamics of proteins, *Protein Dynamics, Methods Protoc* (2014) 193–226.
- [51] I. Kufareva, R. Abagyan, Methods of protein structure comparison, *Homology Modeling: Methods Protoc* (2012) 231–257.
- [52] F. Pan, N. Zhou, J. Li, X. Du, L. Zhao, C. Wang, et al., Identification of C-phycoerythrin-derived peptides as angiotensin converting enzyme and dipeptidyl peptidase IV inhibitors via molecular docking and molecular dynamic simulation, *ES Food Agrofor* 2 (2020) 58–69.
- [53] J. Zhu, H. Li, Y. Xu, D. Wang, Construction of fucoxanthin vector based on binding of whey protein isolate and its subsequent complex coacervation with lysozyme, *J. Agric. Food Chem.* 67 (10) (2019) 2980–2990.